

# Self-Assembling in Nafion Perfluorinated Ionomers Based on ESR Spectra of Novel Fluorinated Nitroxide Spin Probes

Ileana Dragutan,<sup>†</sup> Jayesh G. Bokria, Biji Varghese, Ewa Szajdzinska-Pietek,<sup>‡</sup> and Shulamith Schlick\*

Department of Chemistry, University of Detroit Mercy, Detroit, Michigan 48219

Received: January 31, 2003; In Final Form: July 10, 2003

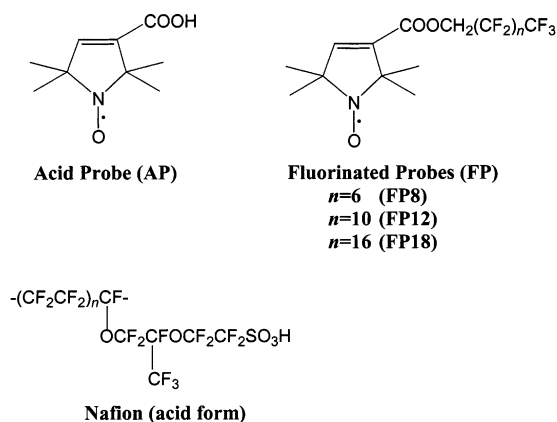
ESR spectra of three fluorinated nitroxide radicals with different lengths of the fluorinated side chain were measured in neat solvents and in aqueous Nafion solutions and membranes swollen by water. The probes were prepared by condensation of the 3-carboxy-2,2,5,5-tetramethyl-3-pyrrolin-1-yloxy acid chloride (acid probe, AP) with 1H,1H-perfluoroalkanol,  $\text{CF}_3(\text{CF}_2)_n\text{CH}_2\text{OH}$ , where  $n = 6, 10, \text{ and } 16$ . The corresponding notation for the probes is FP8, FP12, and FP18. The  $^{14}\text{N}$  hyperfine splittings ( $A_{zz}$  and  $a_N$ ) are sensitive to the local site:  $A_{zz}$  in the range 33.3–36.5 G and  $a_N$  in the range 13.95–16.48 G were measured for solvents ranging from perfluorinated *n*-hexane to 10 M LiCl/water solution. The line shapes in the probe solutions at and near 300 K are sensitive to the presence of oxygen; exceptionally narrow signals (peak-to-peak width 0.1 G) were detected in carefully deaerated probe solutions, thus allowing the measurement of small hyperfine splittings (typically 0.24 G) from the methyl protons. ESR spectra of the fluorinated probes in Nafion solutions and membranes suggested the presence of multiple sites where the probes exhibited a range of dynamics. A possible reason for this effect is the location of probes in a range of amorphous phases where the dynamics is restricted by the proximity to crystalline polymer domains. The  $A_{zz}$  values for the “slow” component of the probes in Nafion solutions and in membranes swollen by water indicated the location of the nitroxides in polar sites, where the local polarity is similar to that in the 10 M LiCl/water system. Probes with longer fluorinated segments penetrate deeper into the assembled polymer chains, farther away from the interface between the polymer aggregate and the solvent. Structural information that can be deduced from protiated and fluorinated probes intercalated in Nafion systems was compared, based on present results and previous studies.

## Introduction

Self-assembling of ion-containing polymers, as swollen membranes and in solutions, was extensively studied in recent years by ESR spectroscopy of nitroxide radicals as spin probes.<sup>1–7</sup> The most important spin probes used were the amphiphilic *n*-doxylstearic acids (*n*DSA) and their corresponding methyl esters (*n*DSE), hydrophobic doxyl-substituted hydrocarbons such as 5-doxyldecane (5DD) and 10-doxylnonadecane (10DND), and cationic probes with different lengths of the alkyl substituents (CAT*n*). The spin probe method is based on the sensitivity of the nitroxide ESR line shapes to the local environment and of the  $^{14}\text{N}$  hyperfine splittings to the polarity of the medium.<sup>8</sup> Depending on probe hydrophobicity, charge, length of the alkyl chain, and, in the case of amphiphilic probes, position of the nitroxide group with respect to the polar headgroup, different regions of self-assembled systems were identified and studied. The ESR spectra of the probes are a rich source of information on local properties such as viscosity, molecular packing and ordering, polarity, and the presence of ions in the probe vicinity, on a nanoscale range, typically 0.5–5 nm.

Some of the probes mentioned above have been used for a comparative study of the protiated ionomer poly(ethylene-co-

**CHART 1. Source Nitroxide (Acid Probe, AP), Fluorinated Probes (FP), and Nafion**



methacrylic acid) (EMAA) neutralized by  $\text{Na}^+$  and  $\text{K}^+$ <sup>2–4</sup> and Nafion perfluorinated ionomer (Chart 1) neutralized by  $\text{Li}^+$ ,<sup>1,5,9,10</sup> as water swollen membranes and in aqueous solutions. Small-angle X-ray and neutron scattering experiments, SAXS and SANS respectively, have clearly indicated the aggregation of ionomer chains into rodlike aggregates of diameter  $\approx 5$  nm and length  $> 40$  nm in Nafion solutions and the reverse micellar structure of swollen membranes, where the solvated ionic clusters are surrounded by the hydrophobic polymer matrix.<sup>11,12</sup> The ESR spectra of the nitroxide probes in Nafion and EMAA

\* Corresponding author. E-mail: schlicks@udmercy.edu.

<sup>†</sup> On leave from The Romanian Academy of Sciences, Institute of Organic Chemistry “C. D. Nenitescu”, Bucharest, Romania.

<sup>‡</sup> Permanent address: The Institute of Applied Radiation Chemistry, Technical University of Lodz, Lodz, Poland.

have been in agreement with the scattering results and have provided additional local details on the aggregates.

Beyond general structural characteristics, the ESR spectra have revealed important differences between EMAA and Nafion systems. In the case of EMAA micelles, probes based on doxylstearic acid have exhibited the "dipstick effect": Their dynamics became slower as the probe penetrated deeper inside the aggregate, from the more hydrophilic *n*DSA to the more hydrophobic *n*DSE and from 5DSA or 5DSE to 10DSA or 10DSE. The  $^{14}\text{N}$  hyperfine splitting,  $a_{\text{N}}$ , decreased in the same order, indicating a polarity gradient from the polar interface to the nonpolar aggregate interior.<sup>2,3,6</sup>

In the case of Nafion micelles, the mobility also decreased in the order 5DSA > 10DSA > 10DSE, but all three probes reported a polar environment.<sup>9,10</sup> The decreased mobility was explained by assuming that the probes intercalate between perfluorinated polymer chains; the high polarity at the probe site was thought to be a result of the water present inside the micelles. This explanation was supported by results of a fluorescence study using pyrene (P) as a polarity probe.<sup>5,13</sup> The fluorescence spectrum of excited P in an aqueous Nafion solution was consistent with the high polarity at the probe site (high-intensity ratio of the first to the third emission peaks) and with the presence of fluorine atoms in its neighborhood (blue shift with respect to the spectrum for P in water). Results obtained for the cationic probes CAT*n* have also indicated the penetration of the protiated segments of the probe inside the perfluorinated host aggregates and have suggested that the amount of water in Nafion micelles increases in more dilute ionomer solutions.<sup>5</sup>

The comparative spin probe ESR study of EMAA and Nafion solutions led to the conclusion that while in the EMAA aggregates the protiated hydrophobic probes (*n*DSE, P) are located in the micellar core, in Nafion aggregates the probes prefer hydrated sites in the palisade region just below the interface rather than the hydrophobic environment of perfluorinated chains. Perfluorinated chains are significantly more hydrophobic than protiated chains, as measured by the lowering of the surface tension of water and the lower critical micelle concentration (cmc).<sup>7,14</sup> The incompatibility between protiated and perfluorinated surfactants has been evidenced in numerous studies; mixtures of hydrocarbon and fluorocarbon surfactants in water are known to demix into hydrocarbon-rich and fluorocarbon-rich micelles for certain solution compositions.<sup>14</sup> In a recent study, this incompatibility has been detected in a mixture of a perfluorinated polymeric surfactant (perfluoropolyether, PFPE) and a protiated surfactant (*n*-dodecylbetaine), in which betaine micelles coexisted with mixed betaine-PFPE vesicles. The results have suggested that the protiated nitroxide probes are located in and report on the dynamics in betaine-rich domains in the vesicles; some conclusions were based on the study of a perfluorinated nitroxide radical derived from PFPE.<sup>15</sup> The spectroscopic studies were confirmed by electron microscopy, which also showed that the composition and size distribution of the aggregates depend on the concentration ratio of the two surfactants.<sup>16</sup>

Recently ESR spectra of a fluorinated nitroxide, 4-(perfluorooctanoyloxy)-2,2,6,6-tetramethylpiperidine-*N*-oxyl (F-TEMPO) have been measured and the  $a_{\text{N}}$  values of the probe were determined in protiated and in perfluorinated surfactants and compared with the corresponding values for the protiated analogue, H-TEMPO. The  $a_{\text{N}}$  values of the fluorinated nitroxide were slightly lower than for H-TEMPO; the difference varied in the range 0.19–0.82 G.<sup>17</sup> This study has also indicated that

the solubility of the fluorinated probe is much higher in a fluorinated surfactant compared to a protiated surfactant and that the difference in solubility increases with increase in the surfactant concentration.

The results in the literature and those of our work on protiated and fluorinated systems encouraged us to examine the behavior of fluorinated spin probes in fluorinated hosts. Such studies are not always easy to perform, since the fluorinated nitroxide radicals are not commercially available. For this study three probes of the general formula presented in Chart 1 were synthesized, and their ESR spectra were examined in a number of solvents and in Nafion systems. The main objectives of this study were to assess the sensitivity of the probes to the local environment in terms of dynamics and range of the magnetic parameters and to determine their ability to report on the structure and dynamics in aqueous solutions of Nafion and in membranes swollen by water.

## Experimental Section

The fluorinated probes with the general formulas given in Chart 1 were synthesized by spin labeling commercially available 1H, 1H-perfluoroalknols,  $\text{CF}_3(\text{CF}_2)_n\text{CH}_2\text{OH}$ .<sup>18–20</sup> The notation used is FP8 (*n* = 6), FP12 (*n* = 10), FP18 (*n* = 16), as shown in Chart 1. The fluorinated alcohol with *n* = 6 was purchased from Aldrich, and the alcohols with *n* = 10 and *n* = 16 from Fluorochem USA, West Columbia, SC.

The precursor paramagnetic acid, 3-carboxy-2,2,5,5-tetramethylpyrrolin-1-yloxy (AP, Chart 1), as well as its corresponding acid chloride were synthesized according to published procedures.<sup>18</sup> Spin labeling of each fluorinated alcohol was then carried out through acylation with excess of AP-acid chloride, in dry ethyl ether and pyridine as the organic base. The acid chloride was prepared immediately prior to reaction, from AP and thionyl chloride in the presence of pyridine, either in situ or separately.

**Synthesis of FP12.** A solution of thionyl chloride (0.2 mL) in dry ethyl ether (15 mL) was added dropwise to a suspension of the acid probe AP (0.4 g) in pyridine (0.3 mL) and dry ethyl ether (10 mL) stirred under ice cooling. The reaction mixture was then stirred in ice for an additional 1 h and at room temperature for 2 h. Pyridine hydrochloride was filtered with suction under argon and washed with ethyl ether, and the filtrate containing AP-acid chloride was transferred into a dropping funnel. The filtrate was added dropwise to a solution of 1H,1H-perfluorododecanol (1 g) in dry ethyl ether (20 mL) and pyridine (0.4 mL). The reaction mixture was stirred under ice cooling for 30 min and then at room temperature overnight. Pyridine hydrochloride was filtered off and the filtrate evaporated in vacuo. The crude product was purified by column chromatography on neutral alumina, using as the eluent gradient hexanes–ethyl ether mixtures, to give 0.4 g of FP12 as yellow needles, mp 95–98 °C.

**Synthesis of FP18.** The same amount of AP-acid chloride, prepared as above, was added dropwise to a stirred solution of 1H,1H-perfluorooctadecanol (1.5 g) in dry ethyl ether (20 mL) and pyridine (0.4 mL), cooled in an ice bath. The reaction mixture was stirred under ice cooling for 30 min and then at room temperature overnight. The procedure resulted in 0.45 g of FP18 as pale yellow crystals, mp 81–85 °C. The purities of both FP12 and FP18 were checked by IR and elemental analysis. The synthesis of FP8 was carried out as reported earlier.<sup>19</sup>

Nafion 117 membranes with an equivalent weight of 1100 g of polymer/mol of  $\text{SO}_3\text{H}$  and a thickness of 0.178 mm were obtained from DuPont. They were pretreated as described

earlier<sup>21</sup> and fully neutralized by  $\text{Li}^+$ . The aqueous Nafion solution containing 5% w/w polymer was obtained by dialysis against water of an ethanol/water Nafion solution prepared from the membrane in an autoclave.

Stock solutions of the probes were prepared in methylene chloride or ethanol; proper amount of this solution was transferred to vials, and the solvent was evaporated under nitrogen. The film thus obtained was then stirred with the neat solvent or solvent mixture, the aqueous Nafion solution, or the membrane suspended in water. The probe concentration in the examined solutions was  $\leq 0.5$  mM, unless otherwise indicated. Probe solutions were prepared in the glovebox under nitrogen, sealed there with Parafilm or Teflon tape, and flame sealed. Additional details on sample preparation have been published.<sup>9</sup>

ESR spectra were recorded with a Bruker X-band EMX spectrometer operating at 9.7 GHz with 100 kHz magnetic field modulation and equipped with the Acquisit 32 Bit WINEPR data system version 3.01 for acquisition and manipulation and the ER 4111 VT variable-temperature unit. The microwave frequency was measured with a Hewlett-Packard 5350B microwave frequency counter. Most spectra were collected with the following parameters: sweep width 120 G; microwave power 2 mW; time constant 40.96 ms; conversion time 81.92 ms; 4–16 scans; 1024–2048 points. Modulation amplitudes in the range 0.5–2 G were used, depending on the line width of the spectrum. The small proton hyperfine splittings were obtained from spectra acquired with sweep width 7 G (covering the low-field  $^{14}\text{N}$  signal), 2048 points, and 0.05 G modulation amplitude.

## Results and Discussion

**ESR Spectra of the Fluorinated Spin Probes in Neat Solvents.** To establish the sensitivity of the magnetic parameters, especially of  $a_{\text{N}}$ , to the local environment, ESR spectra of the fluorinated probe solutions in various solvents within a range of dielectric constants were first measured. The spectra in the organic solvents were extremely sensitive to the presence of oxygen, and extra care was needed in order to obtain maximum resolution. At 300 K the spectra are motionally narrowed; in most solvents  $a_{\text{N}}$  does not depend on the length of fluorinated side chain, within  $\pm 0.05$  G. The  $a_{\text{N}}$  variation in ethanol solutions was however larger, and  $a_{\text{N}}$  values of 15.23, 14.89, and 14.96 G were measured for FP8, FP12, and FP18, respectively, for similar probe concentrations and acquisition parameters; we have no explanation of this effect at present time. Selected spectra for FP12 in neat solvents and solvent mixtures are shown in Figure 1.

In all solvents hyperfine splittings from protons were detected. A typical case is shown in Figure 2, for FP8 in DMF at 300 K. The spectrum was acquired with modulation amplitude 0.05 G. The simulation of the spectrum by assuming hyperfine splittings from 12 equivalent protons is superimposed on the experimental spectrum. The simulation was performed with line width of 0.10 G for the low-field signal of the  $^{14}\text{N}$  triplet, and 0.09 G for the corresponding  $^{13}\text{C}$  satellites. The fit is excellent for the middle region but not as good for the periphery; part of the problem may be the line width variation of the signals, which was not considered in the simulation. The exceptional spectral resolution seems to be typical of this class of probes, as also detected for the AP probe (spectrum not shown). In a recent paper<sup>20</sup> the effect of deuteration was shown for this class of probes; it was reported that the line width for the AP probe (protiated) in degassed benzene at 295 K is 1.03 G, and deuteration reduces the line width to 0.2 G. We believe that the line widths are intrinsically

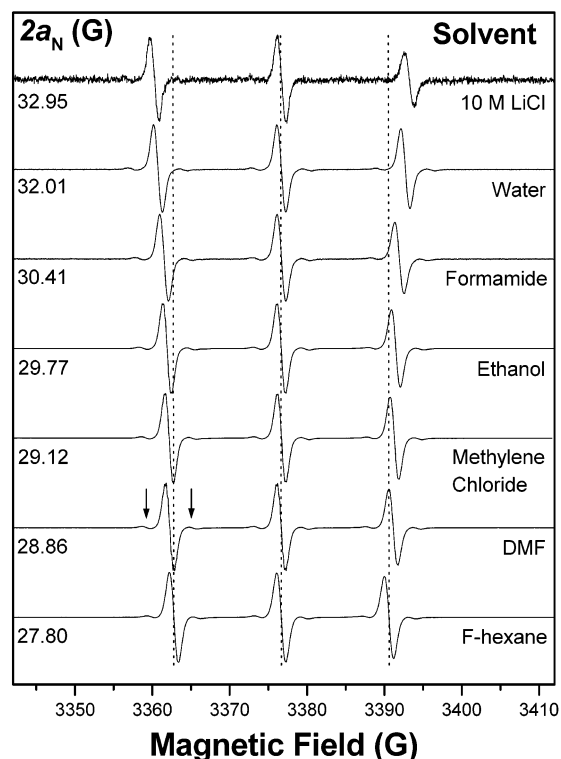


**Figure 1.** X-band ESR spectra at 300 K of the fluorinated probe FP12 in the indicated solvents. Corresponding values of  $2a_{\text{N}}$  in each solvent are indicated; the  $a_{\text{N}}$  values are within  $\pm 0.03$  G. Vertical dotted lines emphasize the  $2a_{\text{N}}$  variation. Downward arrows point to the low-field  $^{13}\text{C}$  signals.

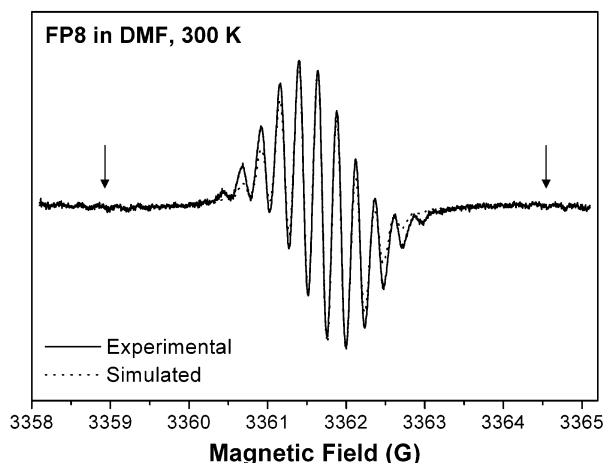


**Figure 2.** ESR spectrum of FP8 in DMF at 300 K (modulation amplitude 0.05 G). The solid line is the low field signal, and the dotted line is the corresponding simulation based on the interaction of the unpaired electron with 12 methyl protons. The main line was simulated with proton hyperfine splitting,  $a_{\text{H}}$ , of 0.24 G and a line width of 0.10 G; the parameters for the  $^{13}\text{C}$  satellites (shown by arrows) were 6.03 G for  $a_{\text{C13}}$ , 0.23 G for  $a_{\text{H}}$ , and 0.09 G for the line width.

very narrow and this effect can be fully visualized only when the oxygen is carefully removed. The line width we have measured for carefully deaerated benzene solution of FP12 at 295 K was 0.13 G. The maximum resolution depends on the temperature, most likely because of spin rotation.<sup>22</sup> The most resolved spectra were detected in DMF, at 280 K for AP and in the range 290–300 K for FP12. Even in water, where oxygen solubility is lower than in organic solvents, broadening by oxygen was detected, and maximum resolution was obtained only in carefully deaerated samples. The results presented here indicate that the line widths are narrow even in protiated probes

**TABLE 1: Magnetic Parameters for the Fluorinated Nitroxide Spin Probe FP12 in Different Solvents:  $^{14}\text{N}$  Isotropic Hyperfine Splitting,  $a_N$ , Measured at 300 K and  $A_{zz}$  Measured at 120 K (or As Indicated)**

solvent	dielectric constant	$a_N$ , G	$A_{zz}$ , G
perfluorinated <i>n</i> -hexane		13.95	33.3
<i>n</i> -hexane <sup>a</sup>	2.0	13.97	
toluene	2.4	14.25	
benzene <sup>b</sup>	2.3	14.24	
dimethylformamide	36.4	14.43	33.8 <sup>b,c</sup>
methylene chloride <sup>a</sup>	8.9	14.56	
ethanol	24.5	14.89	34.05
methanol	32.4	15.02	35.7
formamide	109.0	15.21	
glycerol/water 1:6 v/v		15.98	35.4
water	78.5	16.01	
10 M LiCl/water <sup>d</sup>		16.48	36.5 <sup>c</sup>

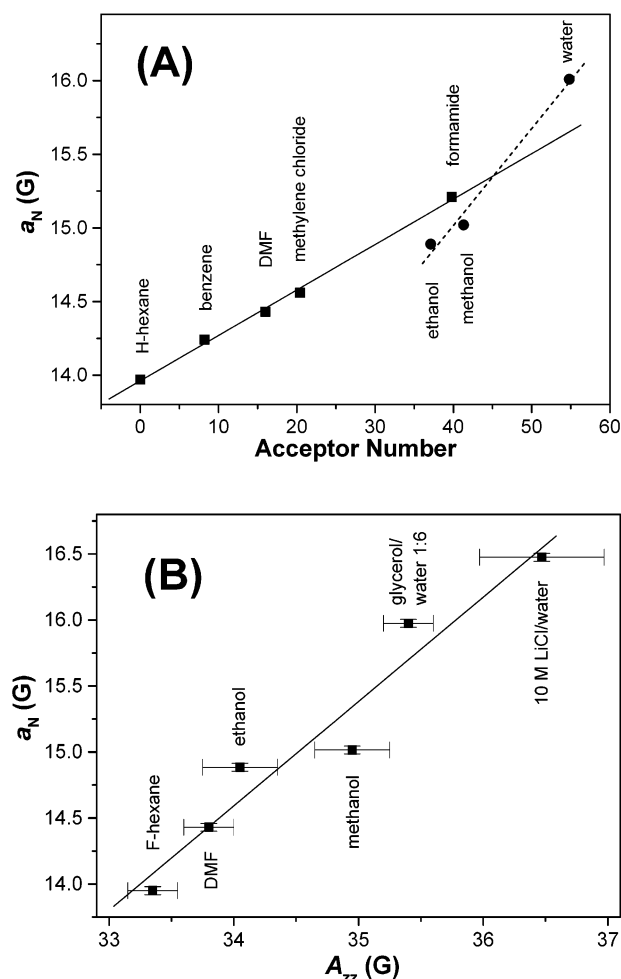
<sup>a</sup> Broad signal at 120 K;  $A_{zz}$  could not be measured. <sup>b</sup> The spectrum at 120 K was not well resolved. <sup>c</sup> Data for FP8. <sup>d</sup> Measured at 100 K.

and there is no need to deuterate, but it is necessary to control the oxygen content. The resolution was also a function of the probe concentration, and concentrations as low as 62  $\mu\text{M}$  were needed for best results. Utilization of these probes for oximetry is suggested, especially in perfluorinated systems such as surfactants and perfluoropolyethers (PFPE).<sup>7a</sup>

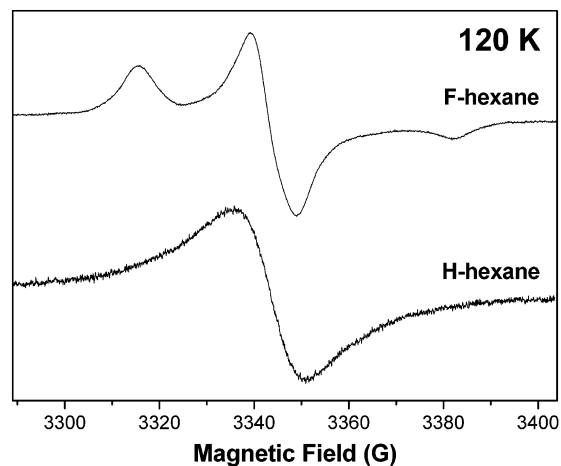
The effects of microwave power saturation, modulation amplitude, and unresolved superhyperfine interactions on the line widths of nitroxide probes have been considered recently by Robinson et al.<sup>23</sup> This approach has been used to simulate the ESR spectrum of nitroxide probe CTPO (3-carboxamide-2,2,5,5-tetramethylpyrrolin-1-yloxy); this probe differs from the AP probe (Chart 1) only in the replacement of the  $-\text{COOH}$  group by  $-\text{CONH}_2$ . The line width determined by simulation of the experimental spectrum presented in Figure 2 of ref 23a (including all corrections) is 0.102 G, compared to 0.10 G used in the simulation presented in Figure 2 of the present paper. We note that even including all corrections, the fit of the spectrum in ref 23a is not perfect, especially in the wings.

Table 1 summarizes  $a_N$  values measured at 300 K for FP12 solutions (unless otherwise indicated). The wide range of  $a_N$  values, 13.95–16.48 G, suggests that these fluorinated nitroxides are good candidates as probes of local environment. It is important to note that there is no correlation between  $a_N$  values and the solvent dielectric constant. As in the case of *n*DSA probes,<sup>24</sup>  $a_N$  values correlate well with the acceptor number of the solvent, an empirical parameter introduced by Mayer et al., which is a measure of the inductive effect of the solvent on the electron density in the solute molecule.<sup>25</sup> This correlation is shown in Figure 3A for solvents of known acceptor numbers. We note that the data for methanol, ethanol, and water deviate from the linear dependence observed for other solvents, an effect that may be due to strong hydrogen bonding. It is interesting to mention that  $a_N$  values for protiated *n*-hexane (H-hexane) and perfluorinated *n*-hexane (F-hexane) are identical within experimental error. In Figure 3B we present the correlation between the principal value of the  $^{14}\text{N}$  hyperfine splitting tensor,  $A_{zz}$ , measured at 120 K for some systems and  $a_N$  measured at 300 K. A reasonably linear dependence is obtained, as expected.<sup>8</sup>

The spectra for FP12 in H-hexane and F-hexane at 120 K are shown in Figure 4. The signal in H-hexane is broad; we exclude the possibility of micellization of the probe in the protiated medium, as the probe concentration was very low, and no evidence for micellization was observed in the other



**Figure 3.** (A) Variation of  $a_N$  for FP12 in the indicated solvents with the acceptor number of the solvent. Separate best fits were drawn for solvents capable of H-bonding (dotted line) and for the rest of the solvents. (B) Correlation between  $A_{zz}$  and  $a_N$  for the indicated solvents. The  $A_{zz}$  values were measured at 120 K, with the exception of 10 M LiCl/water as solvent, which was measured at 100 K. The  $A_{zz}$  value for 10 M LiCl/water solution is given for FP8. The straight line is the best fit to the experimental points.



**Figure 4.** ESR spectra at 120 K of FP12 in perfluorinated *n*-hexane (F-hexane) and in protiated *n*-hexane (H-hexane). See text for details.

protiated solvents. We suggest that phase separation occurs on cooling in the case of H-hexane and not in F-hexane. This would be consistent with a better compatibility (solubility) of the probe in the fluorinated solvent. Phase separation in mixtures of fluorinated catalysts and “conventional” reactants as the tem-



perature decreases is the basis for convenient separation techniques introduced recently in homogeneous catalytic systems.<sup>26</sup>

**ESR Spectra of Fluorinated Spin Probes in Nafion Systems.** The behavior of the probes in Nafion systems was examined in a wide temperature range, 120–350 K for solutions and 120–400 K for membranes. In solution only FP8 and FP12 were examined; we were unable to dissolve a sufficient amount of FP18 in neat water or in aqueous solutions of Nafion. Figures 5A and 6A present selected spectra for FP8 in Nafion solution (5% polymer w/w) and in Nafion membranes swollen by water, respectively. As in the case of protiated probes,<sup>5,9</sup> rigid limit spectra were observed at 120 K. The extreme separation at 120 K,  $2A_{zz}$ , does not depend on the length of fluorinated segment and is the same for the solution and the membrane,  $73.2 \pm 0.3$  G. This high value is the same as that measured for the fluorinated probes in 10 M LiCl aqueous solution (Figure 3B), indicating a highly polar environment. Rigid limit spectra of the probes in water cannot be obtained because phase separation occurs on cooling, but for the glycerol/water system (1:6 v/v) we have determined  $2A_{zz} = 70.8$  G. The extreme separation is approximately constant up to 200 K in the Nafion systems and decreases at higher temperatures, indicating the increasing mobility of the probe. We note that the outer peaks in the slow motional spectra are very broad, especially above 260 K, suggesting a distribution of probe sites with different local mobilities.

In Nafion solutions a “fast” spectral component appeared at 275 K and increased in intensity as the temperature increases (downward arrows in Figure 5A); this signal represents mobile probe molecules (“fast” component). The contribution of this component at 300 K is  $\leq 2\%$  of the total integrated ESR intensity, and the corresponding  $a_N$  is  $16.16 \pm 0.03$  G, within uncertainty the same for FP8 as for FP12; this  $a_N$  value is slightly higher than that in neat water (16.01 G) and lower than for 10 M LiCl/water (16.48 G). At a given temperature the line widths of the fast component are broader compared to the probe in neat water, indicating the different environment. A similar result was obtained for CAT $n$  probes in EMAA solution and was taken as an indicator for the existence of unimeric micelles formed within one polymeric chain, in equilibrium with large multichain aggregates where most of the probe molecules reside.<sup>5,9</sup> From the vertically expanded spectra in Figure 5A it was possible to detect the presence of the “slow” component representing the probe in large aggregates even at 350 K.

Separate line shapes for the slow component in the spectra of the probe in Nafion solutions were obtained by removing the fast component via spectral titration. The deconvolution was performed using the signal recorded for neat water as the titrant, in which the line separation was numerically increased to match the value observed in the presence of Nafion. The slow components for FP8 and FP12 obtained by deconvolution are shown in Figure 5B for spectra measured at 290 K; the temperature was selected to emphasize the spectral differences between the probes. Comparison of the extreme separation (ES) for the two probes in Figure 5B indicates that the dynamics is slower for FP12 than for FP8. If we make the reasonable assumption that the N–O group is anchored at the micellar surface, as suggested by similar  $2A_{zz}$  values for the two probes and their  $a_N$  value (between water and 10 M LiCl), the results can be interpreted to mean that the longer chain of FP12 penetrates deeper into the aggregates, farther away from the interface between the polymer aggregate and the solvent; the line width is clearly larger for FP12, suggesting a wider

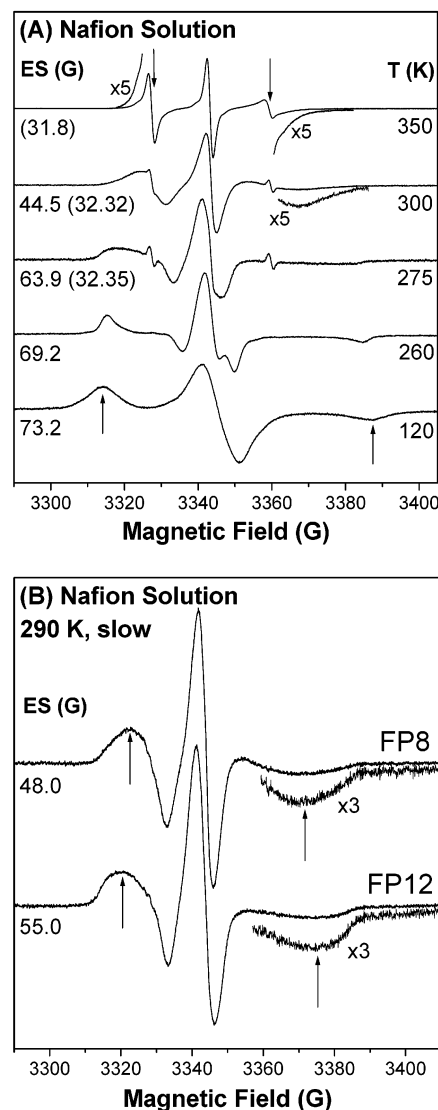


**Figure 5.** (A) ESR spectra at selected temperatures for FP8 in aqueous Nafion solution. The extreme separation (ES) is given on the left:  $2A_{zz}$  in rigid limit spectra (upward arrows) and  $2A_{zz}'$  in slow motional spectra. Numbers in parentheses are the  $2a_N$  values in the motionally averaged regime (downward arrows). (B) Slow motional ESR component for FP8 and FP12 in aqueous Nafion solution at 290 K. Arrows indicate  $2A_{zz}'$  values,  $\pm 0.5$  G. See text for details.

distribution of probe sites. This behavior is reminiscent of that observed for CAT8 versus CAT16 probes in Nafion solutions.<sup>5</sup>

In the Nafion membrane only one spectral component was detected in the examined temperature range (Figure 6A), indicating that the probe is totally incorporated in the polymer domains. The  $2A_{zz}'$  values at a given temperature above 260 K are higher in membrane than in solution, indicating lower probe mobility in the former system. At 360 K the spectrum is almost motionally averaged and  $a_N$  is similar to that measured for the fast component in the solution, 15.9 G, but the signals are significantly broader, suggesting slower dynamics.

Figure 6B presents the ESR spectra at 340 K of the fluorinated probes in Nafion membranes. As in the case of Nafion solutions, the line widths for FP8 are narrower than for FP12, indicating faster rotation. The dynamics of FP18, however, is faster than that of FP12. This result is rather surprising but is consistent with the fact that we were unable to incorporate FP18 in Nafion solutions. Therefore these experiments revealed that increasing

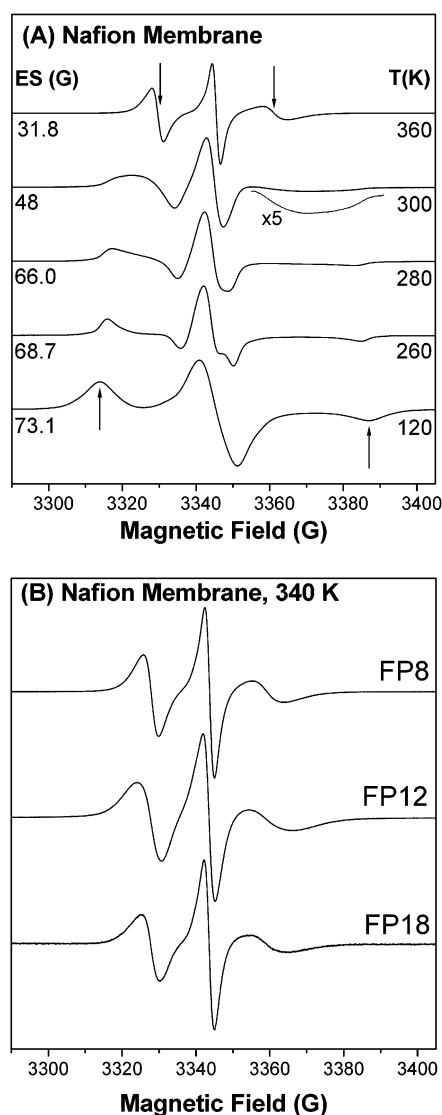


**Figure 6.** (A) ESR spectra at selected temperatures for FP8 in Nafion membrane swollen by water. The extreme separation is given on the left. (B) ESR spectra at 340 K of FP8, FP12, and FP18 in Nafion membrane swollen by water.

the length of fluorinated chain does not necessarily mean deeper penetration of the probe into the Nafion host.

**Effect of Crystalline Domains in Nafion Aggregates.** The line shapes detected for the slow spectral component in Nafion solutions at 290 K (Figure 5B) and in Nafion membrane at 300 K (Figure 6A) are unlike other line shapes detected for the protiated probes in these systems: the outer features are broad, suggestive of a superposition of probe sites. We recall that a multisite model, which assumed a distribution of orientations for the rotational diffusion symmetry axis of the spin probes, has been used to simulate the temperature variation of the spectra for the protiated spin probes 5DSA, 10DSA, and 10DSE.<sup>10</sup> For most spectra five components were added to simulate a given line shape. The line shapes of these protiated probes in the entire temperature range up to 360 K were narrow and the outer features clearly delineated, unlike those for the perfluorinated probes.

We propose that the broad extreme features seen in Figure 5B and in Figure 6A at 300 K are due to probes situated in a range of sites differing in their dynamics because of the proximity to the crystalline domains in Nafion. The situation is analogous to a recent system studied in our laboratory, where

we detected broadening of lines from nitroxide radicals in heterophasic propylene–ethylene copolymers (HPEC) when the degree of crystallinity of the polypropylene component increased.<sup>27</sup> As in the case of HPEC, we propose that in Nafion the probe situated in amorphous domains closer to the crystalline perfluorinated domains are motionally restricted. The broad lines seen in Figures 5 and 6 are taken to represent probes in the *rigid amorphous phase*, which was described in the literature.<sup>28,29</sup> Because the dynamics depends on how close the probe is to crystalline domains, the line shapes represent a gradient in dynamics, which is expected of course to lead to broad outer features at some temperatures.

We now should address the question: do we expect crystalline domains in Nafion aggregates in solution? The first picture of the Nafion micelle in aqueous solution included crystalline domains,<sup>30</sup> but the idea of crystallinity in micelles was abandoned subsequently.<sup>31</sup> Recent results of SAXS and SANS experiments on a range of Nafion concentrations, for volume fractions in the range 0.16–0.95 measured in a wide range of scattering vectors, however, introduced a novel idea of Nafion organization, based on the aggregation of ionomer chains into elongated polymer bundles, surrounded by the electrolyte solution.<sup>32,33</sup> In this model the long rodlike micellar aggregates detected in Nafion solutions are the basic units that aggregate further to form the Nafion membrane. A crucial argument relevant for the line shapes discussed above is that the crystallinity that is known to exist in Nafion membranes also exists in the aggregates in solutions. These recent studies appear therefore to provide support for our explanation of the motionally restricted dynamics and gradient in the probe dynamics.

**Comparison of Protiated and Fluorinated Probes in Nafion.** ESR spectra of both protiated and fluorinated probes reflect a polar environment in aqueous solutions of Nafion and in Nafion membranes swollen by water. The two types of probes are localized in two environments in Nafion solution (slow and fast spectral components), but only in the large aggregates (slow component) in the membranes. The existence of small unimeric or oligomeric micelles in Nafion solutions, which was proposed with reservation in the study of the protiated probes *n*DSA and *n*DSE because of the similar  $a_N$  values in water and in Nafion solutions,<sup>1,5,9</sup> is confirmed by the results of the fluorinated probes.

Besides these similarities, there are subtle but important differences between the behavior of the two types of probes. The calibration of the local polarity in the Nafion systems on the basis of the data for solutions of the fluorinated probes in various solvents (Figures 1 and 3, and Table 1) allowed the more precise determination of the locations for FP8 and FP12: in the polar regions close to the ionic groups. The distinction between FP8 and FP12 is clearly seen in Figure 5B: FP12 is located deeper inside the micelle and explores a wider range of sites, possibly as a result of its higher solubility compared to the protiated probes and its position with respect to crystalline domains. The wide range of sites explored by the fluorinated probes is also evident in the broad lines detected for the Nafion membranes, clearly seen in the ESR spectrum at 300 K, Figure 6A.

The solubilization of FP18 in the membrane and not in the solution of Nafion emphasizes the structural difference between the organization of the chains in the two media: the continuous polymer phase in the membranes assists in the incorporation of the large fluorinated probe but imposes a different conformation. We propose a U-shape conformation for FP18, similar to that

found previously for 16DSA in Nafion/Na membranes<sup>34</sup> and in ionic surfactant micelles and vesicles.<sup>35,36</sup>

## Conclusions

ESR spectra of the fluorinated spin probes shown in Chart 1 were measured in solvents differing in their dielectric constants. The <sup>14</sup>N hyperfine splittings ( $A_{zz}$  and  $a_N$ ) are sensitive to the local site:  $A_{zz}$  in the range 33.3–36.5 G and  $a_N$  in the range 13.95–16.48 G were measured for solvents ranging from perfluorinated *n*-hexane to 10 M LiCl/water solution.

The ESR line widths measured in the probe solutions at 300 K are sensitive to the local concentration of oxygen, and exceptionally narrow signals were detected in carefully degassed samples; for example the line width of FP8 in DMF solutions at 300 K is 0.1 G. The sensitivity of the line shapes to oxygen suggests the possible use of the probes in oxymetry. Narrow line widths were also detected for the precursor, 3-carboxy-2,2,5,5-tetramethylpyrrolin-1-yloxy.

ESR spectra of the fluorinated probes in Nafion solutions and membranes suggested the presence of multiple sites. The  $A_{zz}$  values for the “slow” component of probes in Nafion solutions and membranes suggested their location in highly polar sites, where the polarity is between that in water and in the 10 M LiCl/water system. Comparison of ESR spectra from fluorinated probes indicated that probes with longer fluorinated groups penetrate deeper into the assembled polymer chains. But there is a limit: the longest probe, PF18, cannot be incorporated in the Nafion solutions. The same probe is however solubilized by the Nafion membrane, but the penetration depth is less than that for the probes with shorter perfluorinated chains, possibly due to a U-shape conformation.

The broad outer features in the “slow” spectral component detected in Nafion solutions and in the spectrum of the probes for the membrane at 300 K were explained by assuming a rigid amorphous phase where the probe dynamics is restricted by the proximity to crystalline domains.

**Acknowledgment.** This study was supported by grants from the Polymers Program and International Division (U.S.–Romania) of the National Science Foundation. E.S.-P. is grateful to KBN for partial support of her stay in Detroit. We thank G. Gebel (CEA, Grenoble, France) for the preparation of the Nafion solution and DuPont for donation of the Nafion membrane. We are grateful to the reviewers for their careful reading of the manuscript and useful comments and for bringing to our attention three important references.

## References and Notes

- (1) Szajdzinska-Pietek, E.; Schlick, S. In *Ionomers: Characterizations, Theory, and Applications*; Schlick, S., Ed.; CRC Press: Boca Raton, FL, 1996; Chapter 7, pp 135–164, and references therein.
- (2) Kutsumizu, S.; Hara, H.; Schlick, S. *Macromolecules* **1997**, *30*, 232.
- (3) Kutsumizu, S.; Schlick, S. *Macromolecules* **1997**, *30*, 2329.
- (4) Szajdzinska-Pietek, E.; Pillars, T. S.; Schlick, S.; Plonka, A. *Macromolecules* **1998**, *31*, 4586.
- (5) Szajdzinska-Pietek, E.; Wolszczak, M.; Plonka, A.; Schlick, S. *Macromolecules* **1999**, *32*, 7454.
- (6) Kutsumizu, S.; Goto, M.; Yano, S.; Schlick, S. *Macromolecules* **2002**, *35*, 6298.
- (7) (a) Martini, G.; Ristori, S.; Visca, M. In *Ionomers: Characterizations, Theory, and Applications*; Schlick, S., Ed.; CRC Press: Boca Raton, FL, 1996; Chapter 10, pp 219–250, and references therein. (b) Ristori, S.; Martini, G.; Schlick, S. *Adv. Colloids Interface Sci.* **1995**, *57*, 65.
- (8) *Spin Labeling. Theory and Application*; Berliner, L. J., Ed.; Academic Press: New York, San Francisco, London, 1976.
- (9) Szajdzinska-Pietek, E.; Schlick, S.; Plonka, A. *Langmuir* **1994**, *10*, 1101.
- (10) Szajdzinska-Pietek, E.; Pilar, J.; Schlick, S. *J. Phys. Chem.* **1995**, *99*, 313.
- (11) Gebel, G.; Loppinet, B. In *Ionomers: Characterization, Theory, and Applications*; Schlick, S., Ed.; CRC Press: Boca Raton, FL, 1996; Chapter 5, pp 83–106.
- (12) (a) Gebel, G.; Loppinet, B.; Hara, H.; Hirasawa, E. *J. Phys. Chem. B* **1997**, *101*, 3980. (b) Loppinet, B.; Gebel, G.; Williams, C. E. *J. Phys. Chem. B* **1997**, *101*, 1884.
- (13) (a) Szajdzinska-Pietek, E.; Wolszczak, M.; Plonka, A.; Schlick, S. *J. Am. Chem. Soc.* **1998**, *120*, 4215. (b) Gebel, G. *Polymer* **2000**, *41*, 5829.
- (14) (a) Kissa, E. *Fluorinated Surfactants*; Surface Science Series No.50; Marcel Dekker: New York, 1994; and references therein. (b) Mukerjee, P.; Yang, A. Y. S. *J. Phys. Chem.* **1976**, *80*, 1388. (c) Asakawa, T.; Hisamatsu, H.; Miyagishi, S. *Langmuir* **1995**, *11*, 478. (d) Asakawa, T.; Hisamatsu, H.; Miyagishi, S. *Langmuir* **1996**, *12*, 1204.
- (15) Ristori, S.; Maggiali, C.; Appell, J.; Marchionni, G.; Martini, G. *J. Phys. Chem. B* **1997**, *101*, 4155.
- (16) Rossi, S.; Göran, K.; Ristori, S.; Martini, G.; Edwards, K. *Langmuir* **2001**, *17*, 2340.
- (17) Zhou, J.; Chen, S.; Duan, H.; Jiang, M.; Zhang, Y. *Langmuir* **2001**, *17*, 5685.
- (18) Rozantsev, E. G. *Free Nitroxyl Radicals*; Plenum Press: New York, 1970.
- (19) Dragutan, I.; Dragutan, V.; Caragheorghopol, A.; Zarkadis, A. K.; Fischer, H.; Hoffmann, H.; *Colloids Surf., A* **2001**, *183–185*, 767.
- (20) Radner, F.; Rassat, A.; Hersvall, C.-J. *Acta Chem. Scand.* **1996**, *50*, 146.
- (21) Bednarek, J.; Schlick, S. (a) *J. Am. Chem. Soc.* **1990**, *112*, 5019. (b) *J. Am. Chem. Soc.* **1991**, *113*, 3303.
- (22) Caragheorghopol, A.; Schlick, S. *Macromolecules* **1998**, *31*, 7736.
- (23) (a) Robinson, B. H.; Mailer, C.; Reese, A. W. *J. Magn. Reson.* **1999**, *138*, 199. (b) Robinson, B. H.; Mailer, C.; Reese, A. W. *J. Magn. Reson.* **1999**, *138*, 210.
- (24) Szajdzinska-Pietek, E.; Schlick, S.; Plonka, A. *Langmuir* **1994**, *10*, 2188.
- (25) Mayer, U.; Gutman, V.; Gerger, W. *Monatsh. Chem.* **1975**, *106*, 1235.
- (26) Bradley, D. *Science* **2003**, *300*, 2023.
- (27) Kruczala, K.; Varghese, B.; Bokria, J. G.; Schlick, S. *Macromolecules* **2003**, *36*, 1899.
- (28) Cheng, S. Z. D.; Wunderlich, B. *Macromolecules* **1988**, *21*, 789.
- (29) (a) Wunderlich, B. *Thermal Analysis*; Academic Press: Boston, MA, 1990. (b) Wunderlich, B. *Prog. Polym. Sci.* **2003**, *28*, 383.
- (30) (a) Aldebert, P.; Dreyfus, B.; Gebel, G.; Nakamura, N.; Pineri, M.; Volino, F. *J. Phys. (Paris)* **1988**, *49*, 2101. (b) Gebel, G. Ph.D. Thesis, Université Joseph Fourier, Grenoble, France, 1989.
- (31) Schlick, S.; Gebel, G. In *Ionomers: Characterizations, Theory, and Applications*; Schlick, S., Ed.; CRC Press: Boca Raton, FL, 1996; Chapter 8, pp 165–186.
- (32) Rollet, A.-L.; Diat, O.; Gebel, G. *J. Phys. Chem. B* **2002**, *106*, 3033.
- (33) Rubatat, L.; Rollet, A.-L.; Gebel, G.; Diat, O. *Macromolecules* **2002**, *35*, 4050.
- (34) Lee, K. H.; Schlick, S. *Polym. Prepr. (Am. Chem. Soc. Div. Polym. Chem.)* **1989**, *30*, 302.
- (35) Bratt, P.; Kevan, L. *J. Phys. Chem.* **1992**, *96*, 6849; **1993**, *97*, 7371.
- (36) Jones, R. R. M.; Maldonado, R.; Szajdzinska-Pietek, E.; Kevan, L. *J. Phys. Chem.* **1986**, *90*, 1126.